SEMINAR C TRANSDUCERS

On a family of high-power transducers

A.P. HULST

Philips Research Laboratories, Eindhoven, The Netherlands

In this paper a piezoelectric ultrasonic transducer of the Langevin type is described and analysed. This type of transducer may have its design frequency between 15 and 150 kHz. It can handle a power intensity of more than 40 W/cm^2.

First, the considerations leading to the choice of a symmetrical prestressed design are summarized. A theoretical analysis is then made of the electro-mechanical properties of the unloaded vibrator. The derived formulae for the transformation factor and for the electrical impedance as a function of frequency are experimentally verified. Finally, the analytical results are applied to an acoustically loaded transducer.

Introduction

The principal demands made upon a power transducer for macrosonic applications such as metal and plastic welding, drilling, wire drawing, and cleaning are:

1) It must convert electric power into a certain amount of mechanical vibrational power at the design frequency;
2) the internal power loss must be small, as dissipation is the limiting factor in determining the power to be transferred;
3) the electric impedance must be low, so that a minimum electric voltage is required, and matching to a solid state power source is facilitated; and
4) the design should enable easy loss free coupling of the transducer to the rest of the vibrator.

In order to enable the selection of optimum materials and dimensions for a transducer the quantitative influence of these factors on the electro-mechanical characteristics of the device have to be analysed.

In the present paper, the results obtained from an analysis of the mechanically unloaded transducer are generalized for the loaded transducer by using a two-port representation.

By this means, it is also made possible to determine the varying mechanical properties of the load by means of measurements made at the electrical terminals of the vibrator. This possibility is likely to be most helpful in the study of ultrasonic technological processes.

A piezoelectric sandwich transducer

Design considerations

A few years ago a power transducer was designed which aimed at the fulfilment of the requirements summed up in the Introduction [1]. This transducer, shown in Fig. 1, was designed as a 'sandwich' transducer, consisting of two piezoelectric rings fixed between two metal end pieces. A first advantage of this Langevin [2] type of transducer is the reduction in the length of piezoelectric material required if the device is to resonate at a given frequency [3]. As a result the electric impedance is reduced and the influence of variations in the physical properties of the piezoelectric material on the transducer characteristics is diminished.

A second advantage of the sandwich design is that it makes possible the introduction of a mechanical compressive prestress in the assembly by means of a central bolt [3, 4, 5] or a peripheral sleeve [6]. Thus, the admissible dynamic stress amplitude and hence the maximum power intensity are considerably increased.

Further, the prestress improves the mechanical contact between the parts, which results in a distinct decrease in mechanical damping in the contact zones. The effect is strengthened by the presence of very soft annealed copper shims between the parts.

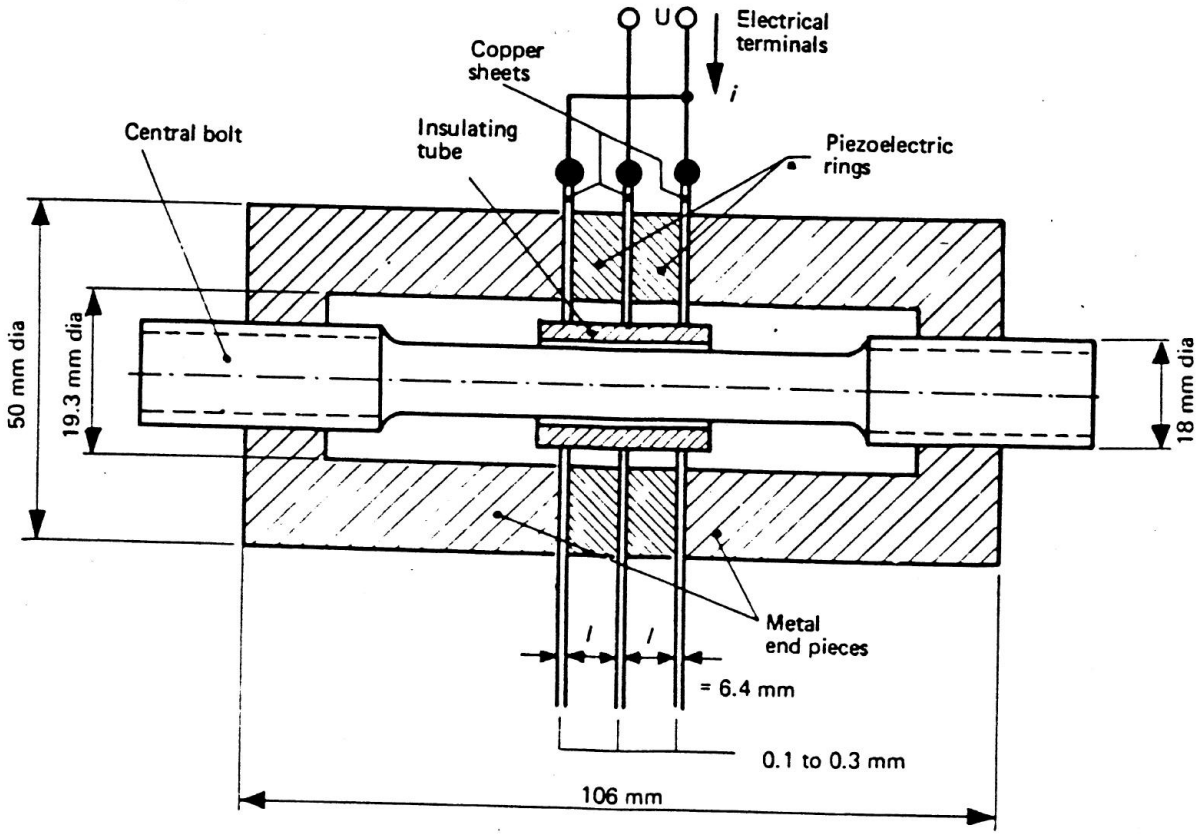

Fig. 1 Composite prestressed ultrasonic transducer (20 kHz version)

Construction

The members of our transducer family are meant to transmit ultrasonic energy from one of their end faces into a solid or liquid load, while the other end face radiates into the air. The piezoelectric rings, which are silver electroded at the end faces, are clamped between the metal end pieces by means of a bolt which bears a permanent tensile stress. The protruding parts of the bolt provide an excellent means of fastening any further waveguide. The bolt is made of the same material as the end pieces in order to avoid friction in the thread between the parts. For the same reason, the dynamic strains in the threaded parts of end piece and bolt are made equal. Therefore, the bolt has its excursion antinode coincident with that of the outer part of the assembly. This has been realized by giving the central bolt a stepped cylindrical form. Langevin's equation [5] has been used to establish the dimensions of the bolt.

The piezoelectric material is the ceramic PZT 4 [7]. The metal parts are made of a titanium alloy. This metal combines a high static and dynamic strength with a low characteristic impedance and a low mechanical loss factor.

The optimum value of the prestress has been established experimentally. Fig. 2 shows how the resonance frequency of the assembly depends on the value of the prestress in the piezoelectric material. At low stress, there is insufficient mechanical contact between the members so that a transition zone of apparently reduced stiffness is present. If the prestress is increased to 35 N/mm^2 the influence of this region has almost disappeared. Also the equivalent damping resistance (see below) is strongly reduced at the higher prestress values [6, 8].

Analysis of the unloaded transducer

The impedance of the freely vibrating transducer

The simplified transducer construction of Fig. 3 is taken as a starting point for the analysis.

As there is symmetry with respect to the plane $z = l + l'$ and as there are no external forces working on the vibrator it follows that:

$$v_D = -v_B \quad \text{and} \quad v_C = 0 \tag{1}$$

where v represents the peak value of the sinusoidally varying particle velocity $v\,(z,t)$. If it is assumed that there is no energy dissipation in the end piece metal, the mechanical driving point impedance of the metal rod BE in $z = l'$ is equal to [9]:

$$Z_m = \mathrm{j}A\,\varrho' c' \tan\left(\frac{\omega l'}{c'}\right). \tag{2}$$

Hence, the peak mechanical stress, σ_E, in the contact plane of ceramic and metal is:

$$\sigma_E = \mathrm{j}\varrho' c' v_E \tan\left(\frac{\omega l'}{c'}\right). \tag{3}$$

As the thickness l of the piezoelectric ring is small compared with the wavelength in the material, the velocity distribution may be linearized in the axial, or 3–, direction. The axial strain S_3 then becomes:

$$S_3 = \frac{\partial \xi}{\partial z} = \text{constant} = -\frac{\xi_E}{l} = -\frac{v_E}{\mathrm{j}\omega l} \tag{4}$$

Here, the velocity v is obtained by multiplying the excursion amplitude ξ with a factor $j\omega = j2\pi f$. If the mechanical stress in the piezoelectric ring, σ_3, is also supposed to be independent of z, it follows by combination of Equations 3 and 4 that:

$$\sigma_3 = \sigma_E = \varrho' c' \omega l S_3 \tan\left(\frac{\omega l'}{c'}\right) = S_3 f(\omega) \qquad (5)$$

with

$$f(\omega) = \varrho' c' \omega l \tan\left(\frac{\omega l'}{c'}\right) \qquad (6)$$

A relation between the mechanical and the electrical quantities in the piezoelectric ceramic is given by the linear piezoelectric relations which, in the general case have the form [10]:

$$S_3 = s^D_{13}(\sigma_1 + \sigma_2) + s^D_{33}\sigma_3 + g_{33}D_3 \qquad (7)$$

$$E_3 = -g_{31}(\sigma_1 + \sigma_2) - g_{33}\sigma_3 + \beta^{\sigma}_{33}D_3 \qquad (8)$$

Here, D_3 and E_3 are the charge density and the electric field strength in the polarization direction, respectively. The constants s^D, g, and β^{σ} are elements of the elastic, the piezoelectric and the dielectric tensors, respectively. As it is not realistic to assume the radial and tangential normal stresses σ_1 and σ_2 to be zero, it is convenient to introduce 'effective' values of the appropriate elastic and piezoelectric constants, viz:

$$\left.\begin{aligned} s^D &= s^D_{33} + s^D_{13}\left(\frac{\sigma_1 + \sigma_2}{\sigma_3}\right) \\ g &= g_{33} + g_{31}\left(\frac{\sigma_1 + \sigma_2}{\sigma_3}\right) \end{aligned}\right\} \qquad (9)$$

Because the sign of $(\sigma_1 + \sigma_2)$ will be opposite to that of σ_3 and because both $s^D_{13} < 0$ and $g_{31} < 0$, it follows that:

$$s^D > s^D_{33} \text{ and } g > g_{33}$$

So, the piezoelectric relations (7) and (8) become:

$$S_3 = s^D \sigma_3 + g_{33}D_3 \qquad (10)$$

$$E_3 = -g\sigma_3 + \beta^{\sigma}_{33}D_3 \qquad (11)$$

Substitution of Equation 5 into 10 yields:

$$\sigma_3 = \left(\frac{g_{33} f(\omega)}{1 - s^D f(\omega)}\right) D_3 \qquad (12)$$

On substitution of this Equation into (11) a relation between the electric field strength and the charge density results:

$$E_3 = \left\{\beta^{\sigma}_{33} - \frac{g\, g_{33} f(\omega)}{1 - s^D f(\omega)}\right\} D_3 \qquad (13)$$

The electric voltage, u, across the transducer terminals equals $E_3 l$ and the summed current intensity in the two

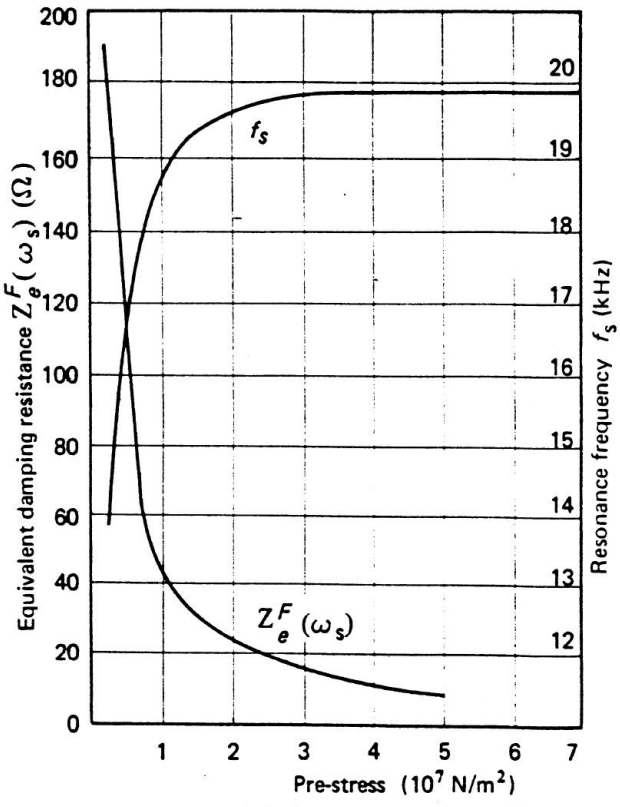

Fig. 2 Influence of the mechanical prestress on the equivalent damping resistance and on the resonance frequency.

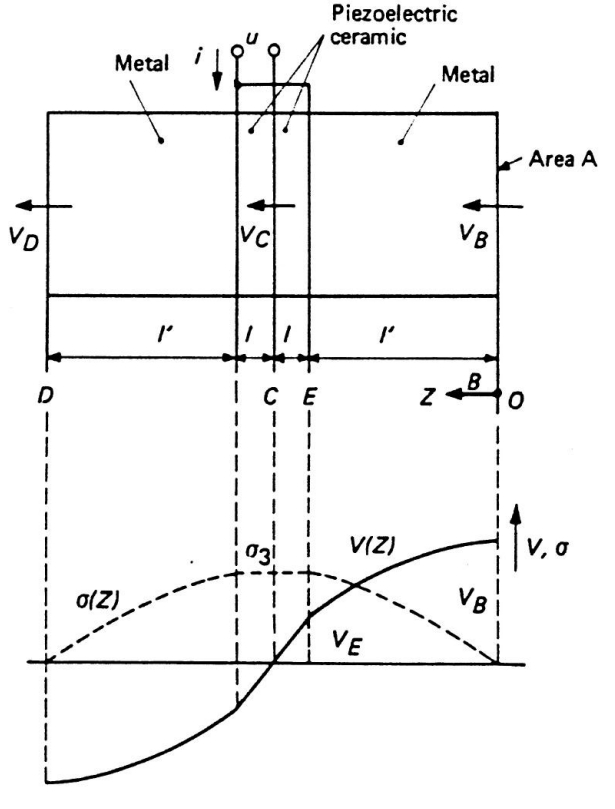

Fig. 3 Distribution of velocity v and stress σ in a simplified transducer.

piezoelectric rings is $j\omega D_3 .2A$. If the capacity C_o is defined as

$$C_o = \frac{2A}{\beta_{33}^{\sigma} l} \quad (14)$$

the electrical impedance at zero mechanical force at the end faces is:

$$Z_e^F = \frac{u}{i} = \frac{1}{j\omega C_o} \cdot \frac{1 - s^E f(\omega)}{1 - s^D f(\omega)} \quad (15)$$

Here, s^E is defined by putting:

$$g.g_{33} = \beta_{33}^{\sigma} (s^E - s^D) \quad (16)$$

by analogy with [7]:

$$g_{33}^2 = \beta_{33}^{\sigma} (s_{33}^E - s_{33}^D)$$

The impedance of the clamped transducer

Consider the imaginary case that the transducer is perfectly clamped at both end faces. Then, analogous to Equation 1 and Fig. 3,

$$F_D = -F_B \text{ and } F_C = 0 \quad (17)$$

Now, the force F is dependent on z in the same way as was the velocity v in the previous section (see Fig. 3). Hence, the mean value of the force in the piezoelectric rings is zero. As the same applies to the stress δ_3, the impedance can be directly derived from Equation 11,

$$E_3 = \beta_{33}^{\sigma} D_3$$

or,

$$Z_e^v = \frac{1}{j\omega C_o} \quad (18)$$

where C_o, the clamped capacitance, is the same as given before in Equation 14. It is noteworthy that the capacitance of the clamped transducer is described by means of the permittivity $1/\beta_{33}^{\sigma}$ at constant stress.

Resonance conditions

The expressions (15) and (18) for the electrical impedance of the transducer remain valid if the coefficients are expressed as complex quantities in order to take account of electrical and mechanical losses. As the mechanical loss factor of the end piece metal is about two orders of magnitude smaller than that of the ceramic, it is assumed that all losses are concentrated in the piezoelectric rings. Hence:

$$\left.\begin{aligned} \underline{s}^D &= s^D (1 - j\delta_m^D) \\ \underline{s}^E &= s^E (1 - j\delta_m^E) \\ \underline{\beta}_{33}^{\sigma} &= \beta_{33}^{\sigma} (1 + j\delta_e) \end{aligned}\right\} \quad (19)$$

The definitions are such that both the mechanical loss factors δ_m and the dielectric loss factor δ_e are positive [11]. By this means, a more general form of the impedance function (15) is obtained:

$$Z_e^F = \frac{1 + j\delta_e}{j\omega C_o} \cdot \frac{1 - \underline{s}^E f(\omega)}{1 - \underline{s}^D f(\omega)} \quad (20)$$

In Fig. 4, the modulus and the phase of the complex impedance are plotted against relative frequency for a typical transducer. Two special frequencies can immediately be derived from Equation 20, viz:

$$f(\omega_s) = \frac{1}{s^E}, \text{ and } f(\omega_p) = \frac{1}{s^D} \quad (21)$$

These formulae define a set of angular frequencies that is comparable to the series and parallel resonance frequencies commonly found in the analysis of vibrators which are entirely made of piezoelectric material [12, 13]. At these angular frequencies, ω_s and ω_p, the impedance is zero and infinite, respectively, if no mechanical losses are present.

For technical purposes it is assumed that:

$$\omega_s \approx \omega_r \text{ and } \omega_p \approx \omega_a \quad (22)$$

where ω_r and ω_a are the frequencies of zero phase difference between electric current and voltage. This assumption holds because the impedances at anti-resonance and resonance differ by more than a factor of 100. The equivalent damping resistance, i.e., the electrical impedance at the resonance frequency ω_s is obtained by substitution of Equation 21 into the impedance function (2),

$$Z_e^F(\omega_s) = \frac{1 + j\delta_e}{j\omega_s C_o} \cdot \frac{j\delta_m^E}{1 - \underline{s}^D f(\omega_s)}$$

or,

$$Z_e^F(\omega_s) \approx \frac{\delta_m^E}{\omega_s C_o k^2} \quad (23)$$

Here, the effective coupling factor is:

$$k^2 = 1 - \frac{s^D}{s^E} \quad (24)$$

The electro-mechanical transformation factor

In the linear case, the electro-mechanical transformation factor T^F is defined as the ratio of the electric current intensity and the mechanical end face velocity of the freely vibrating transducer. Hence, $F = 0$, and

$$T^F = \frac{i}{v_B} \quad (25)$$

where i and v_B are defined as in Fig. 3.

If the complex character of the piezoelectric and mechanical constants is taken into account, Equation 12 is written

$$\delta_3 = \frac{\underline{g}_{33} f(\omega)}{1 - \underline{s}^D f(\omega)} D_3 \quad (26)$$

with $D_3 = i/2j\omega A$. The stress in the piezoelectric ceramic, δ_3, is expressed in the excursion amplitude in the interface E with the aid of Equations 4 and 5.

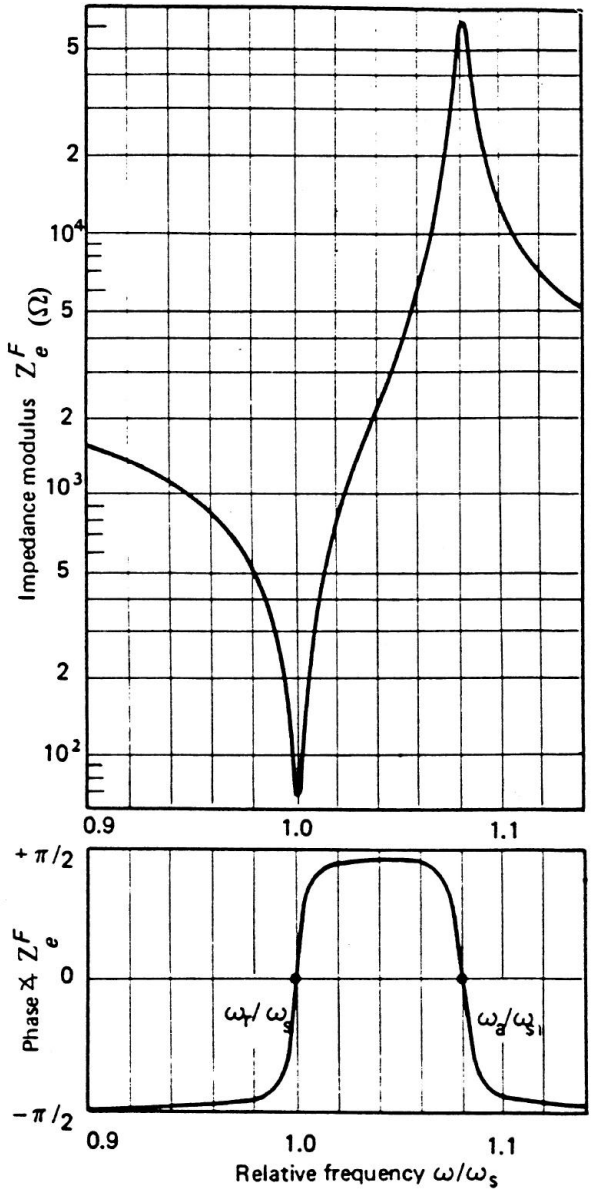

Fig. 4 Modulus and phase of the impedance function (20) for a typical 60 kHz transducer.

$$\vartheta_3 = S_3 f(\omega) = -\frac{\xi_E}{l} f(\omega) = -\frac{v_E}{j\omega l} f(\omega)$$

As the velocity distribution along the z-axis is described with a cosine function, it follows:

$$\vartheta_3 = -\frac{v_B}{j\omega l} \cos\left(\frac{\omega l'}{c'}\right) \cdot f(\omega) \qquad (27)$$

Elimination of ϑ_3 from Equations 27 and 26 yields and expression for T^F, viz:

$$T^F = -\frac{2A}{g_{33} l} \cos\left(\frac{\omega l'}{c'}\right)\left\{1 - \underline{s}^D f(\omega)\right\} \qquad (28)$$

with $f(\omega)$ according to Equation 6, and $\underline{s}^D$ according to Equation (19). Of special interest is the value of T^F at the angular resonance frequency ω_s, where, according to Equations 21 and 24:

$$T^F(\omega_s) = -\frac{2A\,k^2}{\underline{g}_{33} l} \cos\frac{\omega_s l'}{c'} \qquad (29)$$

Verification

It can be seen from relations (18) and (20) that

$$Z_e^F(\omega) \approx \frac{1 + j\delta_e}{jC_o\omega} = Z_e^v(\omega) \text{ if } \omega << \omega_s \qquad (30)$$

This formula is mathematically correct within 0.1% if $\omega < 0.05\ \omega_s$. Hence, if the measuring frequency is taken at about 1 kHz, the capacitance C_0 and the loss angle δ_e are simply measured with the aid of an accurate RCL measuring bridge.

If the quantities s^E, s^D, δ_m^E, δ_m^D, and C_0 of a given ultrasonic power transducer have been determined by substituting the measured data of Table 1 in the relations derived in the present analysis, the frequency response of the impedance function (20) can be computed (see Fig. 4).

The result of such a computation is compared in Fig. 5 with an experimentally determined curve for a 20 kHz transducer. It is found that the computed curve is on average some 2.5 to 5% higher than the measured one, except at the resonance points where the difference, of course, is zero. For 40 kHz and 60 kHz transducers deviations were measured of up to 10%.

The correctness of the derived formulae is clearly shown if the impedance function (20) is combined with Equation 29 in order to obtain an expression for the end face particle velocity, $v(\omega)$, at constant electrical voltage u. Then,

$$v(\omega) = \frac{-j\omega \underline{g}_{33}}{\underline{\beta}_{33}^{\delta} \cos\left(\frac{\omega l'}{c'}\right)\left\{1 - \underline{s}^E f(\omega)\right\}} u \qquad (31)$$

Neglecting the imaginary parts of $\underline{g}_{33}$ and $\underline{\beta}_{33}^{\delta}$, this function is plotted in Fig. 6 along with the results of measurements made on an actual transducer. For these measurements a 'Fotonic Sensor' [14] in conjunction with a lock-in amplifier has been used. In this way, steady state particle velocities can be measured down to 0.2 mm/s at 20 kHz; i.e., an excursion amplitude of about 1.5 nm (15 Ångstrøm). It follows from Fig. 6 that the differences are less than 12% over a dynamic velocity range of a factor of 100, if g_{33} is chosen to fit the measured value $v(\omega_s)$

Discussion

From the data of Table 1 numerical values of a few effective properties of the applied piezoelectric material PZT4 have been computed. These values are collected in Table 2, in comparison with values given by the manufacturer of the material [7].

There are distinct differences between the values of the eleastic compliance s and between those of the constant g_{33}. A positive difference between s and s_{33} was expected previously as shown above. This effect is strengthened by the non-linear character of the stress-strain relationship,

Table 1 Measured electromechanical transducer characteristics

Design frequency	20	40	60	120	kHz
C_o	6.08	1.73	1.18	0.81	nF
ω_p/ω_s	1.059	1.062	1.081	1.045	–
$Z_e^F(\omega_s)$	8.1	54	68	71	Ω
$Z_e^F(\omega_p)$	205	80	63	74	kΩ
$T^F(\omega_s)$	2.4	1.2	0.67	0.27	As/m
$\omega_s l'/c'$	1.276	1.045	1.067	1.251	–

which results in an increasing value of s even at moderate static prestress levels [15]. As s^D appears to be more sensitive to the above-mentioned effects than s^E, the effective coupling factor k is considerably less than k_{33}. The dynamic d_{33} constant may decrease by about 30% if a prestress of 35 N/mm² is applied to a stack of two discs [16]. As $g_{33} = \beta_{33}^{\delta} d_{33}$, and β_{33}^{δ} does not show an appreciable change in our case, a similar behaviour is expected and found for g_{33}.

Although the damping in the end piece metal is very small, the imperfections in the mechanical contact between the constituent parts of the transducer will certainly contribute to the total damping (cf Fig. 2). Hence the values for δ_m^E and δ_m^D must be considered to be upper limits for the inherent damping factor of the piezoelectric material.

The mechanically loaded transducer

Twoport representation

For the application of the analytical results above to the case of the mechanically loaded transducer it is convenient to represent this device as an electro-mechanical twoport. Then electrical voltage u and current intensity i characterize the condition at the electric terminals, while at the mechanical side a force F and a particle velocity v are present. The transfer equations are

$$\left.\begin{aligned} F &= a_{11} v + a_{12} i \\ u &= a_{12} v + a_{22} i \end{aligned}\right\} \qquad (32)$$

The matrix elements a_{ij} are complex functions of frequency. The previously derived transducer characteristics can be expressed in terms of a_{ij}, viz:

$$\left.\begin{aligned} T^F &= \left(\frac{\delta i}{\delta v}\right)^F = -\frac{a_{11}}{a_{12}} \\ Z_e^v &= \left(\frac{\delta u}{\delta i}\right)^v = a_{22} \\ Z_e^F &= \left(\frac{\delta u}{\delta i}\right)^F = a_{22} - \frac{a_{12}^2}{a_{11}} \end{aligned}\right\} \qquad (33)$$

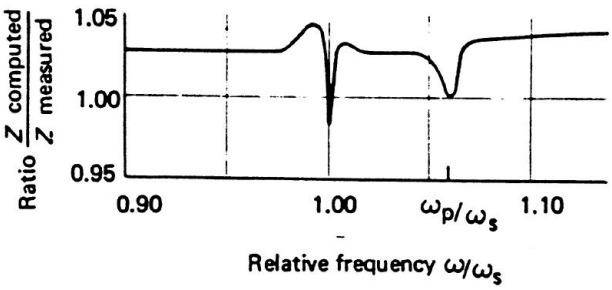

Fig. 5 The ratio between the computed and the measured impedance modulus for a typical 20 kHz transducer.

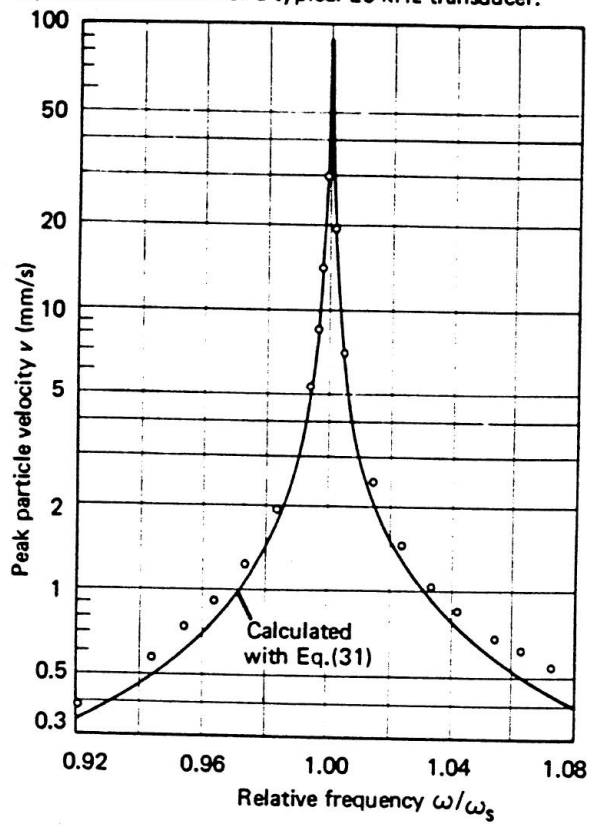

Fig. 6 Comparison of measured and calculated values of the end face particle velocity at a constant voltage of 1 V rms. Typical 20 kHz transducer.

These relations are easily inverted,

$$\left.\begin{aligned} a_{11} &= (T^F)^2 \cdot (Z_e^F - Z_e^v) \\ a_{12} &= T^F \cdot (Z_e^F - Z_e^v) \\ a_{22} &= Z_e^v \end{aligned}\right\} \qquad (34)$$

Analytical expressions for a_{ij} can be obtained upon substitution of the Equations 18, 20 and 28.

Equivalent circuit

The set of Equations (32) is exactly represented by means of the equivalent circuit of Fig. 7. This circuit consists of an electrical branch which is coupled by means of an electromechanical transformer to a mechanical part. In order to satisfy (32) the transformer must have a complex transformer ratio.

Table 2 Effective piezoelectric properties compared with manufacturer's data

Design frequency	20	40	60	120	PZT4	kHz
$1/\beta_{33}^{\delta}$	1.16	1.05	1.20	1.10	1.15	10^{-8} F/m
δ_e	2.5	2.5	2.5	2.5	< 4	10^{-3}
s^E	17.4	21.9	23.3	20.9	15.5*	$10^{-12}m^2/N$
s^D	12.1	17.7	16.6	16.2	7.9†	$10^{-12}m^2/N$
δ_m^E	1.9	4.7	7.8	9.4		10^{-3}
δ_m^D	2.7	6.7	11.3	6.3		10^{-3}
k	0.54	0.44	0.51	0.47	0.7‡	–
g_{33}	19.4	13.4	18.2	19.1	26.1	10^{-3}Vm/N

* s_{33}^E † s_{33}^D ‡ k_{33}

$$N = \frac{a_{12}}{a_{22}} = -A\rho' c' . 2\underline{d}_{33}\omega \sin\left(\frac{\omega l'}{c'}\right) \qquad (35)$$

where $\underline{d}_{33} = \underline{g}_{33}/\underline{\beta}_{33}^{\delta}$. The element $a_{11} - N^2 a_{22}$ represents the mechanical impedance of the transducer for the case of short-circuited electrical terminals,

$$Z_m^u = a_{11} - N^2 a_{22}$$
$$= -jA\rho' c' \sin\left(\frac{2\omega l'}{c'}\right)\left\{1 - \underline{s}^E f(\omega)\right\} \qquad (36)$$

The imaginery part of this impedance,

$$X_m^u = -A\rho' c' \sin\left(\frac{2\omega l}{c'}\right)\left\{1 - \underline{s}^E f(\omega)\right\} \qquad (37)$$

is plotted in Fig. 8a with the quantity $\omega_s l'/c'$ as a parameter. This relation is well approximated in the region $0.9 \leqslant \omega/\omega_s \leqslant 1.1$ by the simple mathematical expression

$$X_m^u \approx A\rho' c' . \pi\left(\frac{\omega}{\omega_s} - 1\right) \qquad (38)$$

If the mechanical branch of the equivalent circuit is supposed to consist of a series connection of mass, spring and damper, as in the usual analysis of entirely piezoelectric vibrators 12, the curve labelled 'IRE-equivalent circuit' in Fig. 8a is then obtained. It is found that relation (38) gives a better approximation of the mechanical reactance in a composite transducer.

The real part of the mechanical impedance follows on substitution of Equation 21 into Equation 36:

$$R_m^u = A\rho' c' \sin\left(\frac{\omega l'}{c'}\right)\delta_m^E . \frac{f(\omega)}{f(\omega_s)} \qquad (39)$$

This function is represented in Fig. 8b. From the analysis it follows that the mechanical damping resistance R_m^u changes about 2% for a frequency deviation of 1%. It follows from Fig. 7 that a low impedance is obtained at the electric terminals for a given acoustic load if N is made high. This means that a high d_{33} constant is a desirable property of the piezoelectric material to be applied.

The transducer under load

In Fig. 9, the equivalent circuit of a complete ultrasonic power-transfer system is given. Here, the electrical branch a_{22} of Fig. 7 is represented by the lossless capacity C_o in parallel with the dielectric loss resistance $R_e = 1/\omega C_o \delta_e$. In general, the load consists of an imaginary part X_{mL} in series with a real part R_{mL} [17]. The output frequency of the ultrasonic power source is adjusted automatically in such a way that the phase difference between output current and voltage is zero. The introduction of a self-inductance $L_o = 1/\omega_s^2 C_o$, which is connected in parallel to the electrical terminals, results in a relatively high impedance of the electrical branch near resonance. Then, the zero phase condition demands that:

$$X_m^u + X_{mL} = 0 \qquad (40)$$

so that the total impedance measured at the electrical terminals is real and minimum.

In conclusion, if a generator is applied, which is equipped with an automatic frequency control system, it is possible to measure both the real and the imaginary part of a varying load at the electrical terminals. The real part is determined from the quotient of voltage and current intensity, whereas the imaginary part is proportional to the difference between the working frequencies under loaded and unloaded conditions.

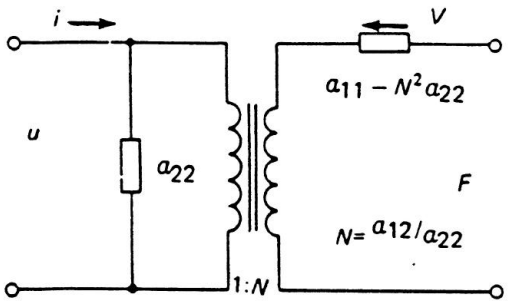

Fig. 7 Equivalent transducer circuit.

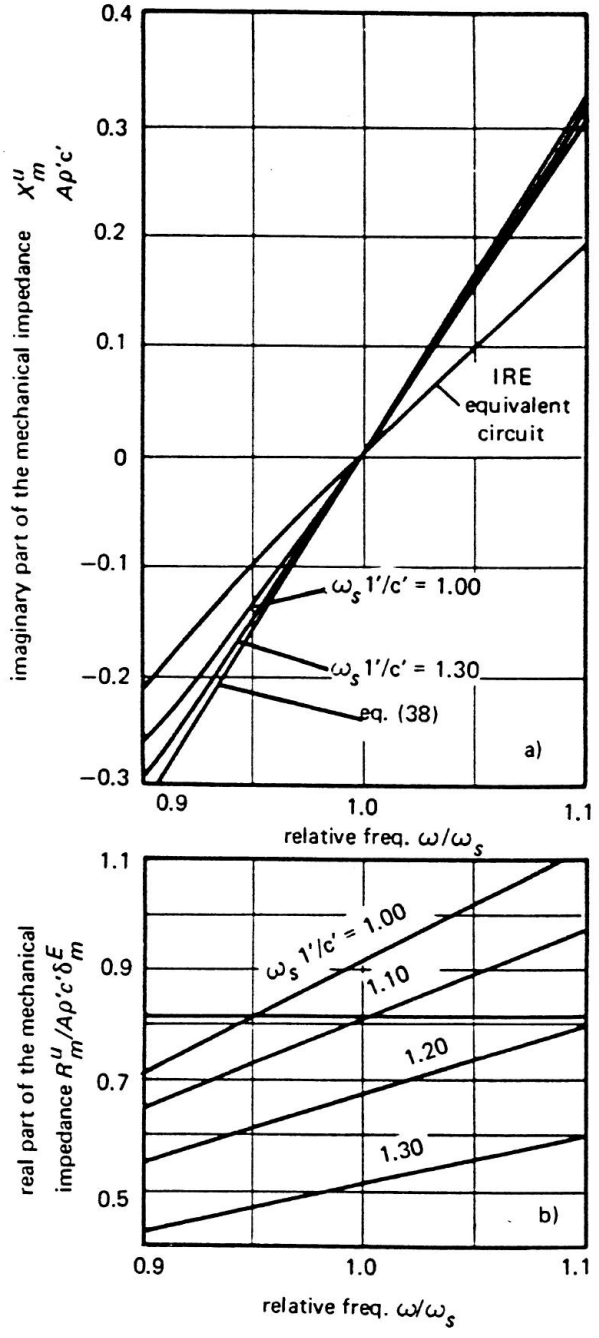

Fig. 8 Representation of the imaginary part (a) and the real part (b) of the mechanical impedance at zero voltage, in comparison with the IRE formulae for single-crystals.

Power, optimum load and efficiency

The reactive electric power in the piezoelectric material per unit volume is given by

$$p_e = \frac{\omega E_3^2}{2\beta^{\sigma}_{33}}$$

if E_3 is the peak value of the electric field strength [18]. A similar expression is valid for the mechanical reactive power

$$p_m = \frac{\omega s^E \sigma_3^2}{2}$$

The sum of the acoustic power delivered to the load and the mechanical power loss in the transducer, i.e., the power to be converted, is defined by means of the effective piezoelectric coupling factor:

$$p_t = k\sqrt{p_e p_m} = \tfrac{1}{2}\omega k E_3 \sigma_3 \sqrt{\frac{s^E}{\beta^{\sigma}_{33}}} = \tfrac{1}{2}\omega E_3 \sigma_3 d_{33}\sqrt{\frac{g}{g_{33}}} \qquad (41)$$

after substitution of the Equations 16 and 24. Hence, the maximum power per unit volume that can be converted by a piezoelectric material at a given frequency is determined by the constant d_{33}, and by the admissible field strength and dynamic stress amplitudes.

If, as an approximation, the factor $(g/g_{33})^{1/2}$ is neglected, it follows that:

$$p_{t\,\max} = \tfrac{1}{2}\omega d_{33} E_{3\,\max} \cdot \sigma_{3\,\max} \qquad (42)$$

The limits on E_3 and σ_3 are generally imposed by heat generation resulting from dielectric and mechanical losses. If $E_{3\,\max} = 2.8$ kV/cm (2 kV_{rms}/cm), $\sigma_{3\,\max} = 20 N/mm^2$ and $d_{33} = g_{33}/\beta^{\sigma}_{33}$ from Table 2 is taken, a value of about 4 W/cm³ kHz for $p_{t\,\max}$ is arrived at, in agreement with literature [19].

The actual stress in the ceramic rings at resonance depends chiefly on the end face velocity of the transducer – see Equations 6 and 27 – so that:

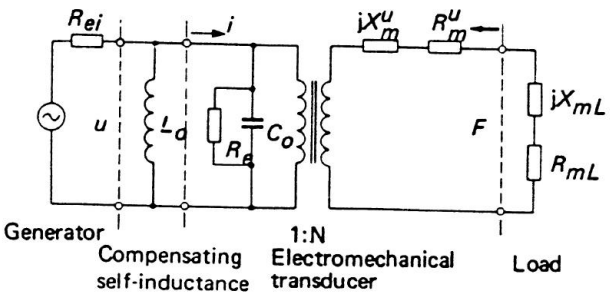

Fig. 9 Complete equivalent circuit of a loaded vibrator

$$v = \frac{-j\,\delta_3}{\rho' c' \sin(\omega_s l'/c')} \quad (43)$$

From the equivalent circuit of Fig. 9 it follows that:

$$E_3 = \frac{u}{l} = \frac{\left(R_m^u + R_{mL}\right) v}{Nl} \quad (44)$$

Then, after substitution of Equations 35 and 43 in Equation 44 it follows that:

$$\left(R_m^u + R_{mL}\right)_{opt} = 2\omega_s A (\rho' c')^2 d_{33} \sin^2\left(\frac{\omega_s l'}{c'}\right) \frac{E_{3max}}{\sigma_{3max}} \quad (45)$$

The real part of the electric impedance is, in the case of the load given in Equation 45,

$$\left(R_e\right)_{opt} \approx \frac{\left(R_m^u + R_{mL}\right)_{opt}}{N^2} = \frac{E_{3max}}{2Ad_{33}\omega_s\,\delta_{3max}} \quad (46)$$

Hence, the optimum electrical impedance is lower according as the area of the piezoelectric rings is greater. If the assumed values of E_{3max} and δ_{3max} are substituted in Equation 45 together with the data of Tables 1 and 2, a general relation is found between the optimum mechanical load resistance and the wave impedance for our type of transducer, viz:

$$\left(R_m^u + R_{mL}\right)_{opt} = (0.08 \text{ to } 0.12)\, A\rho' c' \quad (47)$$

A few power measurements made on the sandwich transducer indicate that indeed the power efficiency [17] is optimum for the load given in Equation 47.

An overall efficiency of 88% at a power intensity of 41 W/cm^2 has been measured at that load.

Conclusions

1) The sandwich type of ultrasonic power transducer described in this paper is well suited for the efficient conversion of electric power into acoustic power at an intensity of at least 40 W/cm^2. The design frequency can be chosen between 15 and 150 kHz.
2) The transducer has a very simple design and is easily coupled to any metallic waveguide system.
3) The electrical impedance under clamped and free mechanical conditions, the electro-mechanical characteristics and the resonance conditions are adequately described by the applied one-dimensional mathematical model.
4) It is possible to determine both the real and the imaginary part of a varying mechanical load in a simple way by measuring electric voltage, current intensity and frequency dynamically at the output terminals of the ultrasonic generator.
5) The principal demands that must be made on a piezoelectric material for high-power applications are:
   a) the mechanical and dielectric loss factors must be low in order to improve efficiency, or, to increase the power handling capacity by enabling the application of high dynamic stress and high electric field strength;
   b) the piezoelectric constant d_{33} must be high in order to improve the power handling capacity and to decrease the electric impedance at a given acoustic load.
6) The volume of a given piezoelectric material determines the total power that can be converted. A minimum value of the optimum electrical impedance under load is obtained if the area of the piezoelectric rings is maximum.

Symbols

A	area of the piezoelectric rings	m^2
C_0	capacitance of the transducer at low frequency	F
c'	velocity of sound in end piece metal	m/s
D_3	charge density in polarization direction	C/m^2
d_{33}	piezoelectric constant = g_{33}/β^q_{33}	m/V
E_3	electric field strength in polarization direction	V/m
f	frequency	Hz
$f(\omega)$	frequency function, Equation 6	N/m^2
g_{33}, g	piezoelectric constant	Vm/N
i	current intensity	A
k	effective piezoelectric coupling factor	–
l	thickness of a piezoelectric ring	m
l'	length of a metal end pieze	m
N	electromechanical transformer ratio, Equation 35	As/m
R_m, R_e	mechanical or electrical resistance	kg/s, Ω
S_3	strain in polarization direction	–
s_{33}, s	elastic compliance	m^2/N
T	electromechanical transformation factor, Equation 25	As/m
u	electric voltage	V
v	particle velocity	m/s
X_m	mechanical reactance	kg/s
Z_m, Z_e	mechanical or electrical impedance	kg/sΩ
β_{33}	inverse dielectric constant	m/F
δ_m, δ_e	mechanical or electrical loss angle	–
ϱ	specific mass of end piece metal	kg/m^3
δ	mechanical stress in polarization	N/m^2
ω	angular frequency = $2\pi f$	s^{-1}
ω_p, ω_s	parallel or series angular resonance frequency	s^{-1}

References

1 Daniëls, H.P.C., Tates, H.K. and van der Ven, T.J. Philips Research Laboratories, Eindhoven.

2 Langevin, P. British Patent 145 691 (1921).

3 Van Randeraat, J. (Editor). *Piezoelectric Ceramics*, N.V. Philips, Gloeilampenfabrieken, Eindhoven, (1968).

4 Enz, U. Dia Erzeugung von Ultraschall mit Ferriten. *Technische Mitteilungen P.T.T.*, 33, 6 (1955), pp. 209-212.

5 Mori, E. and Ueha, S. On the bolt-clamped Langevin type transducer, *Proc. 6th Intern. Congress on Acoustics*, Tokyo, (1968).

6 Jones, J.B. and Maropis, N. Transducer assemby, US Patent 3 283 182 (1966).

7 Berlincourt, D.A., Curran, D.R. and Jaffe, H. Piezoelectric and piezomagnetic materials, *Physical Acoustics*, Vol. I, Part A, Chap. 3, New York, Academic Press, (1964).

8 Mori, E. and Takahashi, S. Measurements of large amplitude vibrational characteristics of ultrasonic power transducers. *Proc. 6th Intern. Congress of Acoustics*, Tokyo, (1968).

9 Snowdon, J.C. *Vibration and shock in Damped Mechanical Systems*. Wiley & Sons, London, (1968).

10 Reference [7], p. 227.

11 Holland, R. Representation of dielectric, elastic and piezoelectric losses by complex coefficients. *IEEE Trans.* SU-14, (1967), pp. 18-20.

12 IRE standards on piezoelectric crystals – the piezoelectric vibrator: definitions and methods of measurement. *Proc. IRE* 45 (1957), pp. 353-358.

13 IRE standards on piezoelectric crystals: measurements of piezoelectric ceramics. *Proc. IRE* 49 (1961), pp. 1161-1169.

14 Mechanical Technology Inc., 968 Albany-Shaker Road, Latham, New York 12110.

15 Berlincourt, D. and Krueger, H.H.A. Domain processes in lead titanate zirconate and barium titanate ceramics. *J. of Applied Physics*, 30, 11 (1959), pp. 1804-1810.

16 Flinn, J and Hulyer, J.P.. Testing piezoelectric ceramics for power transducer applications. *Ultrasonics for Industry*, Iliffe, Guildford, (1969).

17 Hulst, A.P. Macrosonics in industry 2. Ultrasonic welding of metals, *Ultrasonics* 10, 6, (1972), pp. 252-261.

18 Reference [7], p. 250.

19 Maropis, N. The design of high-power ceramic transducer assembly, *IEEE Trans.* SU-16, 3, (1969), pp. 132-136.